Phase Noise Metrology

Fred L. Walls

Total Frequency
Boulder, CO 80303

ABSTRACT

This paper describes the fundamental concepts that characterize the phase modulation (PM) noise and amplitude modulation (AM) noise of electronic devices in the frequency-domain, and their relationship to tradition time-domain measures of frequency stability. The statistical confidence of the data is discussed. Using the fundamental concepts, the affects of frequency multiplication, division, and mixing on PM noise are explored. Also covered is the relationship between noise figure and PM/AM noise in an amplifier. The affect of summing a large number of similar sources or amplifiers on the resulting PM noise is briefly mentioned.

Common techniques used to measure PM noise in oscillators such as single channel two-oscillator, dual channel two-oscillator, three-cornered-hat with cross correlation, delay line discriminator, and carrier suppression are described. It is shown how these techniques can be extended to the measurement of PM noise added by other electronic devices such as amplifiers and frequency multipliers/dividers. Common errors and the strengths and weaknesses of the various measurement and calibration techniques are also described.

Key Words: Phase noise metrology, AM noise, PM noise, frequency stability, jitter.

1. INTRODUCTION

In this paper we review the basic definitions generally used to describe phase modulation (PM) noise, amplitude modulation (AM) noise, fractional frequency stability, timing jitter and phase jitter in precision sources and other devices [1-4]. From these basic definitions we can then compute the affect of frequency multiplication or division on these measures of performance. We find that under ideal frequency multiplication or division by a factor N, the PM noise and phase jitter of a source is intrinsically changed by a factor of N^2 [5,6]. The fractional frequency stability and timing jitter are, however, unchanged as long as we can determine the average zero crossings. After a sufficiently large multiplication factor N, the carrier power density is less than the PM noise power. This is often referred to as carrier collapse [6]. Ideal frequency translation results in the addition of the PM noise of the two sources. The effect of AM noise on the multiplied or translated signals can be increased or decreased depending on the component non-linearity. Noise added to a precision signal results in equal amounts of PM and AM noise. Each component affects the spectrum as described above. The upper and lower PM (or AM) sidebands are exactly equal and 100% correlated, independent of whether the PM (or AM) originates from random or coherent processes [7]. As an example we treat thermal noise added to a precision signal by an amplifier and show the ideal relationship to the noise figure. Unfortunately most amplifiers exhibit white PM noise levels from 1 to 5 dB above that expected from the noise figure in the presence of a large carrier signal due to non-linear intermodulation processes [8,9].

The power spectrum of a signal, such as is obtained with a spectrum analyzer, sums the power in the carrier signal with the AM and PM noise. To differentiate between the various contributions to total power it is necessary to use measurement systems that can discriminate between AM and PM noise. A variety of such measurement systems are discussed with their advantages and disadvantages. Some calibration techniques are also discussed.

2. BASIC DEFINITIONS

2.1 DESCRIPTIONS OF VOLTAGE WAVE FORM

Figure 1 shows the power spectrum of a signal as observed on a typical spectrum analyzer. Note that the power is spread between the fundamental signal and a number of harmonics. Note that there typically are spurious signals on

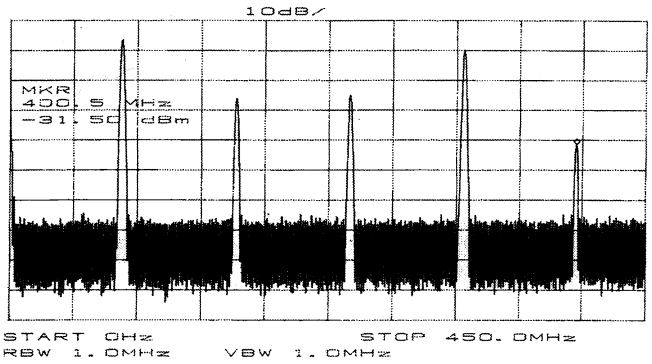

Figure 1. Power spectrum of a signal.

the fundamental at separations that correspond to the power line frequency and its harmonics. There can also be spurious signals that originate from other sources in close proximity to the signal under test, or from a distant source such as a strong radio, TV, or other communication station.

To develop precise notation of what we mean by phase modulation (PM) or amplitude modulation (AM) we need to develop some definitions and mathematical tools [1-4]. The fundamental or harmonics of a precision source can be written as

$$V(t) = [V_o + \varepsilon(t)][\cos(2\pi\nu_o t + \phi(t))], \tag{1}$$

where ν_o is the average frequency, and V_o is the average amplitude. Phase/frequency variations are included in the term $\phi(t)$ and the amplitude variations are included in $\varepsilon(t)$ [2]. The instantaneous frequency is given by

$$\nu = \nu_o + \frac{1}{2\pi}\frac{d}{dt}\phi(t). \tag{2}$$

The instantaneous fractional frequency deviation is given by

$$y(t) = \frac{1}{2\pi\nu_o}\frac{d}{dt}\phi(t). \tag{3}$$

The power spectral density (PSD) of phase fluctuations $S_\phi(f)$ is the mean squared phase fluctuation $\delta\phi(f)$ at Fourier frequency f from the carrier in a measurement bandwidth of 1 Hz. This includes the contributions at both the upper and lower sidebands. These sidebands are exactly equal in amplitude and are 100% correlated [7]. Thus experimentally

$$S_\phi(f) \equiv \mathrm{PSD}[\phi(t)] \equiv \frac{[\delta\phi(f)]^2}{BW} \qquad \mathrm{rad^2/Hz}, \qquad BW \ll f,\ 0 < f < \infty, \tag{4}$$

where BW is the measurement bandwidth in Hz.

Since the BW is small compared to f, $S_\phi(f)$ appears locally to be white noise and therefore obeys Gaussian statistics. The fractional confidence interval for power spectral density measures of white noise is approximated by $1 \pm (\beta/N)^{1/2}$, where β is the 1 for 1-sigma or 62% confidence limit, 2 for 2-sigma or 95% confidence limit, 3 for 3-sigma confidence limit, and N, the number of averages is larger than 10 [10].

PM noise is often specified in terms of single side band noise L(f), which is defined as ½ of $S_\phi(f)$. The units are generally given in dBc/Hz, which is short hand for dB below the carrier in a 1 Hz bandwidth.

$$L(f) = 10 \log[\tfrac{1}{2} S_\phi(f)] \quad \mathrm{dBc/Hz}. \tag{5}$$

Frequency modulation noise is often specified as $S_y(f)$, which is the PSD of fractional frequency fluctuations. $S_y(f)$ is related to $S_\phi(f)$ by

$$S_y(f) = [f^2/\nu_o^2]\, S_\phi(f), \qquad 1/\mathrm{Hz}. \tag{6}$$

Typically $S_y(f)$ is comprised of regions where the noise follows a power law dependence on f. The 5 common noise types are given in Eq. (7) in terms of $S_y(f)$ and $S_\phi(f)$. The coefficients are identified as: h_{-2} is random walk FM, h_{-1} is flicker FM, h_0 is white FM, h_1 is flicker PM, and h_2 is white PM. Most precision sources have at least 3 of these noise types plus aging or drift [1-4].

$$S_y(f) = h_{-2}f^{-2} + h_{-1}f^{-1} + h_0 + h_1 f + h_2 f^2, \tag{7a}$$

$$S_\phi(f) = \nu_o^2[h_{-2}f^{-4} + h_{-1}f^{-3} + h_0 f^{-2} + h_1 f^{-1} + h_2]. \tag{7b}$$

Figure 2 shows a representation of Eqs. (7a) and (7b).

The amplitude modulation (AM) noise $S_a(f)$ is the mean squared fractional amplitude fluctuations at Fourier frequency f from the carrier in a measurement bandwidth of 1 Hz. Thus experimentally

$$S_a(f) = \mathrm{PSD}\left[\frac{\varepsilon(t)}{V_o}\right] \equiv \left(\frac{\delta\varepsilon(f)}{V_o}\right)^2 \frac{1}{BW} \qquad 1/\mathrm{Hz}, \qquad BW \ll f,\ 0 < f < \infty, \tag{8}$$

where BW is the measurement bandwidth in Hz.

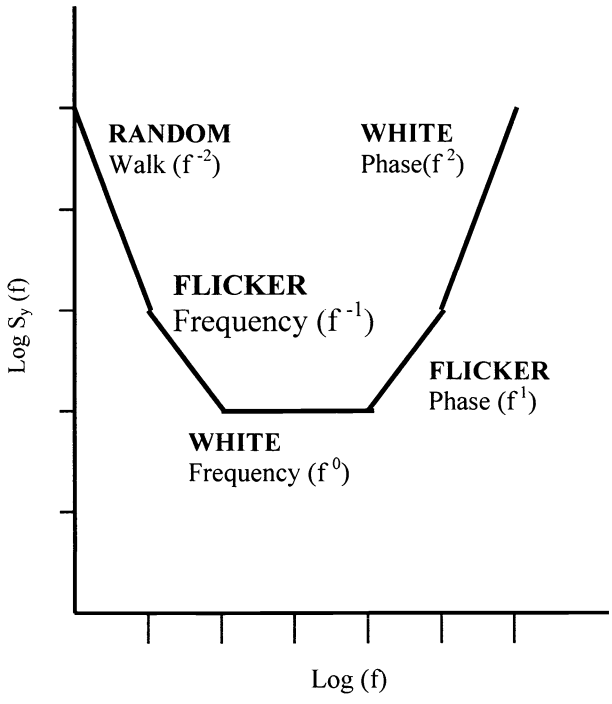

Figure 2a. Log Sy(f) for the 5 common noise types as a function of offset frequency f.

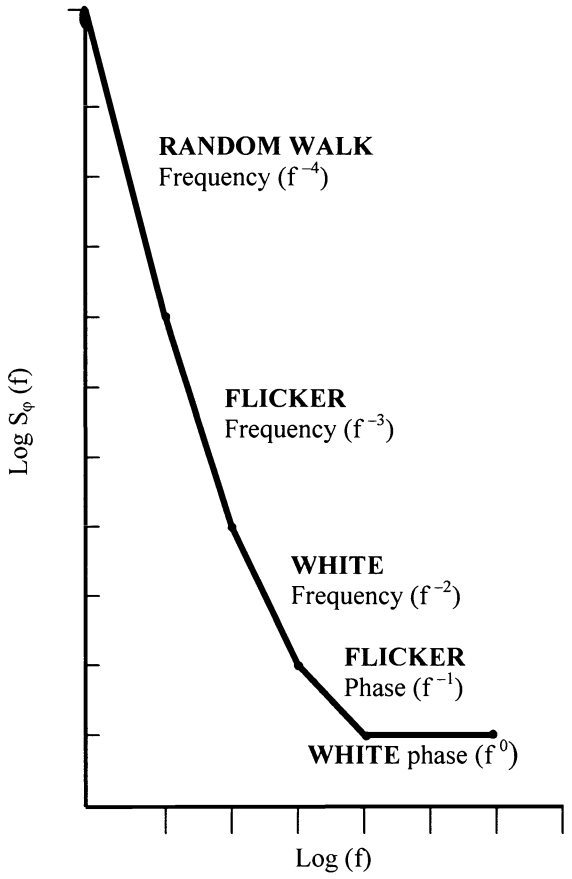

Figure 2b. Log $S_\varphi(f)$ for the 5 common noise types as a function of offset frequency f.

The rf power spectrum for small PM and AM noise is approximately given by

$$V^2(f) \cong V_o^2[e^{-\phi_c^2} + S_\phi(f) + S_a(f)], \tag{9}$$

where $e^{-\phi_c^2}$ is the approximate power in the carrier at Fourier frequencies from 0 to f_c [6]. ϕ_c^2 is the mean squared phase fluctuation due to the PM noise at frequencies larger than f_c [6]. ϕ_c^2 is calculated from

$$\phi_c^2 = \int_{f_c}^{\infty} S_\phi(f)\,df. \tag{10}$$

The half-power bandwidth of the signal, 2 fc can be found by setting $\phi_c^2 = 0.7$. The difference between the half-power and the 3-dB bandwidth depends on the shape of $S_\phi(f)$ [6].

2.2 FREQUENCY STABILITY IN THE TIME DOMAIN

The frequency of even a precision source is not stationary in time, so traditional statistical methods to characterize it diverge with increasing number of samples [1-4, 11, 12]. Special statistics have been developed to handle

this problem. The most common is the two-sample or Allan variance (AVAR), which is based on analyzing the fluctuations of adjacent samples of fractional frequency averaged over a period τ. The square root of the Allan variance $\sigma_y(\tau)$, often called the ADEV, is defined as

$$\sigma_y(\tau) = \left\langle \frac{1}{2}[\bar{y}(t+\tau) - \bar{y}(t)]^2 \right\rangle^{1/2} . \tag{11}$$

$\sigma_y(\tau)$ can be estimated from a finite set of frequency averages of length τ from

$$\sigma_y(\tau) = \left[\frac{1}{2(M-1)} \sum_{i=1}^{M-1} (y_{i-1} - y_i)^2 \right]^{1/2} . \tag{12}$$

This assumes that there is no dead time between samples. If there is dead time, the results are biased depending on type of PM noise. See [13] for details. $\sigma_y(\tau)$ can also be calculated from the $S_\phi(f)$ using

$$\sigma_y(\tau) = \left(\frac{\sqrt{2}}{\pi \nu_o \tau} \right) \left[\int_0^\infty H_\phi(f)[S_\phi(f)] \sin^4(\pi f \tau) df \right]^{1/2} , \tag{13}$$

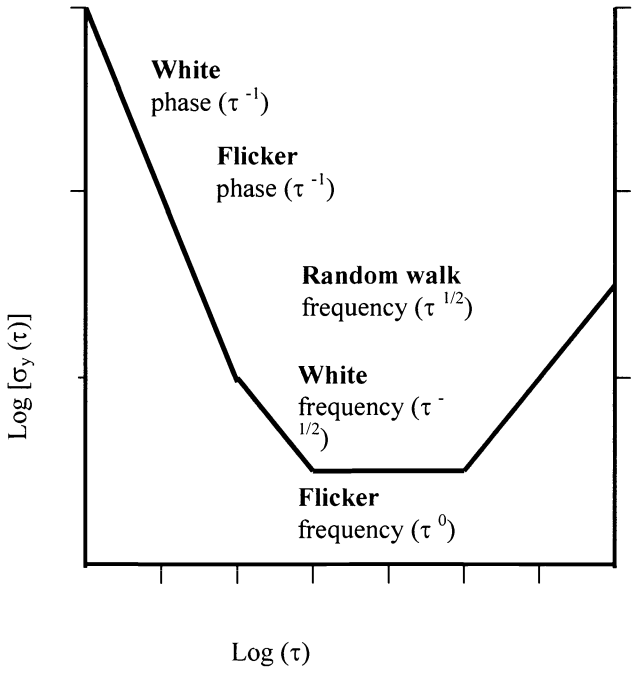

Figure 3. Log $\sigma_y(\tau)$ versus τ for the 5 common noise types

where $H_\phi(f)$ is the transfer function of the system used for measuring $\sigma_y(\tau)$ or δt below. See Fig. 3 and Table 1 [5,14]. If $H_\phi(f)$ has a low pass characteristic with a very sharp roll off at a maximum frequency f_h, it can be replaced by 1 and the integration terminated at f_h. Practical examples usually require the exact shape of $H_\phi(f)$. [14]. Several other statistics have been developed to characterize the statistics of frequency standards [2]. Total deviation is an estimate of the Allan deviation that removes an important bias for sampling times that are longer than 10% of the data length [15]. A nice statistical package that allows one to easily calculate many of these characterizations along with their associated uncertainties is Stable 32 [16].

2.3 PHASE JITTER

The phase jitter $\delta\phi$ is computed from the PM noise spectrum using

$$\delta\phi = \int_0^\infty [S_\phi(f)] H(f) df . \tag{14}$$

Generally H(f) must have the shape of the high pass filter or a minimum cutoff frequency f_{min} used to exclude low frequency changes for the integration, or $\delta\phi$ will diverge due to random walk FM, flicker FM, or white FM noise

processes. H(f) usually has a low pass characteristic at high frequencies to limit the effects of flicker PM and white PM. See Table 1 [5].

2.4. TIMING JITTER

Recall that $\sigma_y(\tau)$ is the fractional frequency stability of adjacent samples each of length τ. The time jitter δt over a period τ is the timing error that accumulates after a period τ. δt is related to $\sigma_y(\tau)$ by

$$\frac{\delta t}{\tau} = \frac{\delta \upsilon}{\upsilon} = \sigma_y(\tau) \qquad \delta t = \tau \sigma_y(\tau). \tag{15}$$

Table 1 shows the asymptotic forms of $\sigma_y(\tau)$, δt, and $\delta\phi$ as a function of Tau, f_{min}, and f_h for the 5 common noise types at frequency υ_o and $N\upsilon_o$ [5]. It is interesting to note that for white phase noise, all three measures are dominated by f_h. For random walk frequency modulation (FM) and flicker FM, $\sigma_y(\tau)$ is independent of f_h and instead is dominated by $S_\phi(1/\tau)$ or $S_\phi(f_{min})$. Also, the timing jitter is independent of N as long as we can still identify zero crossings, while the phase jitter, which is proportional to frequency, is multiplied by a factor N. Typical sources usually contain at least 3 of these noise types.

3. EFFECTS OF FREQUENCY MULTIPLICATION, DIVISION, AND TRANSLATION

3.1 FREQUENCY MULTIPLICATION AND DIVISION

Frequency multiplication by a factor N is the same as phase amplification by a factor N. For example 2π rad is amplified to $2\ \pi$ N rad. Since PM noise is the mean squared phase fluctuation, the PM noise *must* increase by N^2. Thus

$$S_\phi(N\nu_o, f) = N^2 S_\phi(\nu_o, f) + \text{Multiplication PM}, \tag{16}$$

where Multiplication PM is the noise added by the multiplication process.

Table 1. $\sigma_y(\tau)$, δt, and $\delta\phi$ as a function of τ, f_{min}, and f_h at carrier frequency υ_o and $N\upsilon_o$

Noise type	$S_\phi(f)$	$\sigma_y(\tau)$	δt at υ_o or $N\upsilon_o$	$\delta\phi$ at υ_o	$\delta\phi$ at N υ_o
Random Walk FM	$[\nu^2/f^4]h_{-2}$	$\pi[(2/3)h_{-2}\tau]^{1/2}$	$\tau\pi[(2/3)h_{-2}\tau]^{1/2}$	$\upsilon[1/(3f_{min}^3)h_{-2}]^{1/2}$	$N\upsilon[1/(3f_{min}^3)h_{-2}]^{1/2}$
Flicker FM	$[\nu^2/f^3]h_{-1}$	$[2\ln(2)h_{-1}]^{1/2}$	$\tau[2\ln(2)h_{-1}]^{1/2}$	$\upsilon([(1/(2f_{min}^2)h_{-1}]^{1/2}$	$N\upsilon([(1/(2f_{min}^2)h_{-1}]^{1/2}$
White FM	$[\nu^2/f^2]h_0$	$[\{1/(2\tau)\}h_0]^{1/2}$	$[(\tau/2)h_{-0}]^{1/2}$	$\upsilon\{[(1/f_{min}) - (1/f_h)]h_0\}^{1/2}$	$N\upsilon[(1/f_{min}) - (1/f_h)]h_0^{1/2}$
Flicker PM	$[\nu^2/f^1]h_1$	$[1/(2\pi\tau)]\ [1.038 +3\ln(2\pi f_h\tau)h_1]^{1/2}$	$[1/(2\pi)]\ [1.038 +3\ln(2\pi f_h\tau)h_1]^{1/2}$	$\upsilon[\ln(f_h/f_{min})h_1]^{1/2}$	$N\upsilon[\ln(f_h/f_{min})h_1]^{1/2}$
White PM	$[\nu^2 f^2]h_2$	$[1/(2\pi\tau)][3f_h h_2]^{1/2}$	$[1/(2\pi)][3f_h h_2]^{1/2}$	$\upsilon[f_h h_2]^{1/2}$	$N\upsilon[f_h h_2]^{1/2}$

We see from Eqs. (9), (10), and (16) that the power in the carrier decreases exponentially as e^{-N^2}. After a sufficiently large multiplication factor N, the carrier power density is less than the PM noise power. This is often referred to as carrier collapse [6]. Ideal frequency translation results in the addition of the PM noise of the two sources. The half-power bandwidth of the signal also changes with frequency multiplication.

Frequency division can be considered as frequency multiplication by a factor 1/N. The effect is to reduce the PM noise by a factor $1/N^2$. The only difference is that there can be aliasing of the broadband PM noise at the input to significantly increase the output PM above that calculated for a perfect divider [17]. This effect can be avoided by using a narrow band filter at the input or intermediate stages.

3.2 EFFECT OF FREQUENCY TRANSLATION

Frequency translation has the effect of adding the PM noise of the input signal ν_1 and the reference signal ν_o to that of the PM noise in the nonlinear device providing the translation.

$$S_\phi(\nu_2, f) = S_\phi(\nu_o, f) + S_\phi(\nu_1, f) + \text{Translation PM}. \tag{17}$$

Thus dividing a high frequency signal, rather than mixing two high frequency signals, generally produces a low frequency reference signal with less residual noise.

3.3 EFFECT OF ADDITIVE NOISE

The addition of a broadband noise signal $V_n(t)$ to the signal $V_o(t)$ yields a total signal

$$V(t) = V_o(t) + V_n(t). \tag{18}$$

Since the noise term $V_n(t)$ is uncorrelated with $V_o(t)$, ½ the power contributes to AM noise and ½ the power contributes to PM noise.

$$\text{AM } V_n(t)/\sqrt{2} \qquad \text{PM } V_n(t)/\sqrt{2}, \tag{19}$$

$$L(f) = \frac{s_\phi(f)}{2} = \frac{s_a(f)}{2} = \frac{V_n^2(f)}{4V_o^2}\frac{1}{BW}, \tag{20}$$

where BW is the bandwidth in Hz.

These results can be applied to an ideal linear amplifier or detection circuit as follows. The input noise power to the amplifier is given by kTBW. The gain of the amplifier from a matched source into a match load is G_o. The noise power to the load is just $kTBWG_oF$, where F is the noise figure. The output power to the load is P_o. Using Eq. (20) we obtain

$$L(f) = \frac{s_\phi(f)}{2} = \frac{s_a(f)}{2} = \frac{V_n^2(f)}{4V_o^2}\frac{1}{BW} = \frac{2kTBWFG_o}{4P_oBW} = \frac{kTFG_o}{2P_o} = -177\text{dBc/Hz}, \tag{21}$$

for T= 300K, F=1, , $P_o/G_o = P_{in}$ = 0 dBm.

This result differs from some of the literature, but has been experimentally verified [9,18]. Many amplifiers show an increase of the broadband noise, and hence both AM and PM noise, of 1 to 5 dB above (21) as the signal level increases. This effect is due to nonlinear intermodulation processes [8,9]. The effect is very small in ultra linear amplifiers such as those using feed forward technology and in those with low-level signals [9].

3.4 AFFECT OF SUMMING N SOURCES

Some applications could benefit from summing the outputs of a large number of nominally independent sources [19]. In the idealized case where the phase angle between the individual outputs and the summed output are less than 0.1 rad and the amplitudes are all equal, the PM noise of the summed signal is given by

$$L^{\text{Sum}}_{i=1\text{ to }N} = \frac{1}{N^2}\sum_{i=1}^{N} L_i(f), \tag{22}$$

where $L_i(f)$ is the PM noise of the i^{th} source. Note that there is no requirement that the PM noise of each source $L_i(f)$ be equal, or that they have any particular spectral type, for example white PM noise. A similar result also applies to the AM noise of the combined source. In the case where all $L_i(f) = L_o(f)$, equation (22) simplifies to

$$L^{\text{Sum}}_{i=1\text{ to }N} = \frac{1}{N^2}\sum_{i=1}^{N} L_i(f) = \frac{1}{N}L_o(f). \tag{23}$$

In practice this case can only be approximated. Phase shifts between the output of the individual sources and the sum result in a cross coupling of AM noise in the individual sources to PM noise in the sum. This process also cross couples PM noise in the individual sources to AM in the sum. To a much lesser degree the phase shift between the outputs causes a reduction in maximum available output power for the sum. A more serious issue is that to maintain relatively tight phase control of the individual sources using a phase-locked-loop (PLL) to reduce the cross coupling of AM and PM noise, also imposes PM noise from the common reference $L_{ref}(f)$ on the individual sources. This common reference noise does not diminish with the summation. Including these effects, but assuming linear power summation with isolation between the individual sources that is greater than 10 log 3N, we obtain a more realistic result for (23)

$$L^{\text{Sum}}_{i=1\text{ to }N}(f) \cong \left\langle\left|\frac{G(f)}{1+G(f)}\right|^2\right\rangle L_{ref}(f) + \frac{1}{N}\left\langle\left|\frac{1}{1+G(f)}\right|^2\right\rangle\langle L_o(f)\rangle + \frac{1}{2N}\left\langle S_a(f)\{\sin^2[\Theta_i + \Theta_{ni}(f_{BW})]\}\right\rangle, \tag{24}$$

where $\left\langle\left|\frac{G(f)}{1+G(f)}\right|^2\right\rangle$ is the average PLL transfer function for imposing the PM noise of the common reference on the individual sources, Θ_i is the average phase angle and $\Theta_{ni}(f_{BW})$ the noise modulation of the average angle between the i^{th} source and the summed output, and $S_a(f)$ is the average AM noise for the individual sources [19]. To keep the coupling of the AM noise to the PM noise of the summed output at less than –20 dB one must keep $\Theta_i + \Theta_{ni}(f_{BW})$

smaller than 0.1 rad. $\Theta_{ni}(f_{BW})$ depends on the PLL bandwidth. This result does not include environmental effects, which could be common to the individual source. The PLL effects outlined above and explored more in [19] probably explain why significant reductions in PM noise for summed sources at low offset frequencies have yet to be reported in the literature. In an ideal system with negligible PM to AM conversion in the summation process, and good isolation between sources, the AM noise of the summed output is not affected by either AM or PM noise in the reference source.

4. PM NOISE MEASUREMENT SYSTEM

4.1 SINGLE CHANNEL SETUP FOR A PRECISION OSCILLATOR

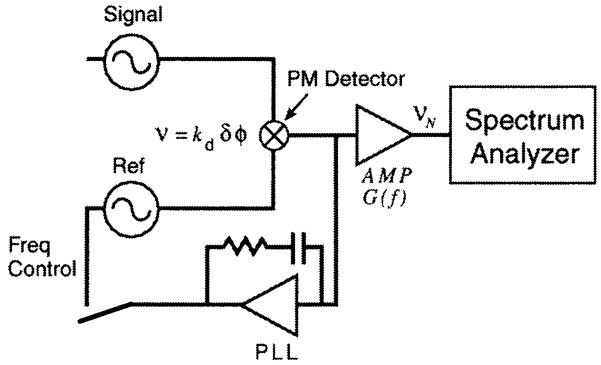

Figure 4a. Block diagram of a simple PM noise measurement system. PSD $V_N/[K_dG(f)] = S_\phi(f)$ of the signal plus that of the Ref and the measurement system.

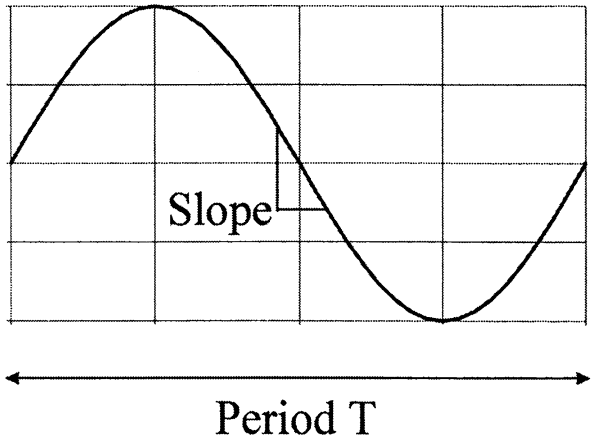

Figure 4b. Beat note from Fig. 4a with PLL open. The slope in rad/volt is equal to the mixer sensitivity multiplied by amplifier gain $[K_dG(f)]$ at the beat frequency

The block diagram of a single channel PM noise measurement system is shown in Fig. 4a [2,4]. Here the signal from a precision oscillator, whose PM noise is to be measured, is mixed with that of a noise reference oscillator with lower PM noise at nominally the same frequency using a mixer, typically a double balanced mixer (DBM). Figure 4b shows the beat between the oscillators when the PLL is open. The slope at the zero crossing has a linear relationship between voltage and phase difference. For phase excursions of less than 0.1 rad from $\pi/2$ (quadrature), the output of the DBM and amplifier has a very linear relationship between voltage and phase difference. In this region we can write the output as

$$V_{out} = K_d \delta\phi, \qquad \text{with } \delta\phi = \Delta\phi - \pi/2, \tag{25}$$

where $\delta\phi$ are the small phase fluctuations between the two oscillators due to the PM noise [2,4,18]. Conventional units for K_d are V/rad. This is a convenient method of converting the phase fluctuations into voltage fluctuations, which are then amplified by G(f) and fed to a spectrum analyzer. The output of the DBM is also passed through an amplifier with a low pass loop filter to the voltage control input of the reference oscillator to hold the output of the DBM near 0 Vdc, thus completing a PLL. This circuit ensures that the phase of the oscillators nominally track each other with a phase difference of $\pi/2$. The power spectral density of PM noise of the oscillator under test is given by Eq. (4) when the PM noise of the reference oscillator, mixer, and the amplifier can be neglected [2,4,18].

$$S_\phi(f) = [V_n(f)/G\,K_d]^2 \; 1/BW \qquad \text{rad}^2/\text{Hz}, \tag{26}$$

where $V_n(f)$ is the rms noise voltage at the Fourier offset frequency f from the carrier in a bandwidth BW. BW must be small compared to f. This is very important where $S_\phi(f)$ is changing rapidly with f, e.g. $S_\phi(f)$ often changes as f^{-3} near the carrier. To determine the conversion sensitivity of the mixer (K_dG) one opens the PLL and adjusts the reference oscillator for a small frequency offset. The resulting beat frequency signal out of the amplifier, which is often clipped due to saturation in the amplifier, is then fed to an oscilloscope or other recording device and the linear slope near its zero crossing is determined. See Fig. 4b. The value of K_d in Volts/rad is then given by

$$K_d\,G = (\Delta V / \Delta T)\,(T_b / 2\pi) \tag{27}$$

This approach determines $K_dG(f)$ only at the beat frequency $1/T_b$. With care $K_dG(f)$ can be made flat to within a few dB over the range of Fourier frequencies from the bandwidth of the PLL circuit up to a few MHz. The effect of the PLL on $S_\phi(f)$ can be measured directly or the gain adjusted to make the bandwidth less than the Fourier frequency of interest. More elaborate calibrations methods described below allow the determination of $K_dG(f)$ over the entire range of interest [2,4,18].

If the oscillators are tuned too closely to one another the phase of one signal pulls the phase of the other. This manifests itself by asymmetric beat signals and in severe cases by synchronization of the two signals. The remedy is to increase the offset and/or the isolation between the signals such that the positive and negative half cycles and the negative and positive going slopes through the zero-crossing are equal to within 10% so that an accurate measurement of $K_dG(f)$ can be made.

Errors in this measurement approach can be caused by frequency dependence of $K_dG(f)$, lack of discrimination against AM in the mixer, bias of the results at low offset frequencies due to the action of the PLL, too much PM noise in the Ref oscillator, and contributions from the noise floor.

4.2 CALIBRATED PM NOISE STANDARD APPROACH

The above method of determining ($K_dG(f)$), although sufficiently accurate for many measurements, is usually time consuming and requires considerable operator skill. A more elegant method of determining [$K_dG(f)$] consists of adding a precisely known noise source PM/AMCAL onto one of the signal inputs of the DBM [4,18-20]. The experimental arrangement is shown in Fig. 5. The PM noise added by PM/AMCAL is such that it is much higher than the sum of those from the input oscillators, mixer and the amplifiers and at the same time not high enough to saturate the spectrum analyzer input. In some configurations, the added noise is constant to within ± 0.1 dB for Fourier frequencies from DC to ≅ ¼ the bandwidth of the band pass filter following the noise source [20]. With the noise source on, the measured power spectral density $V_n(f)_{on}$ is given by PM/AMCAL from which $(K_d\ G(f))^2$ can be determined as a function of f. This corrects for any frequency dependence of K_d or G(f).

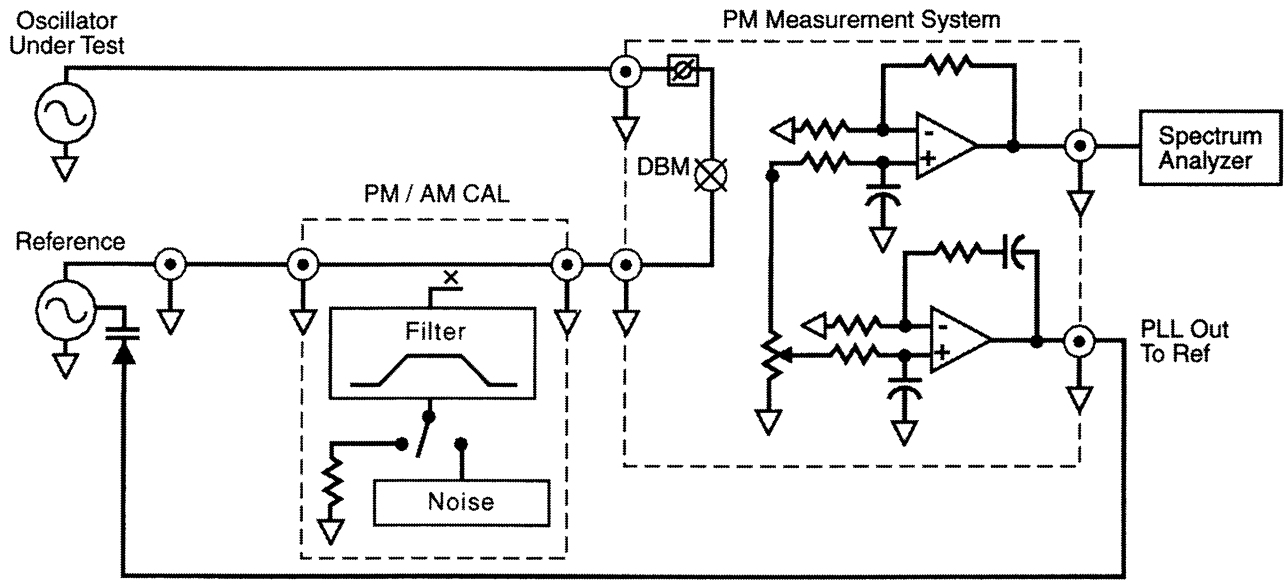

Figure 5. Block diagram of PM noise measurement system for two oscillators with in-situ calibration standard PMAM/CAL to determine the mixer sensitivity and amplifier gain [$K_dG(f)$] as a function of Fourier frequency. PSD V_N /[$K_dG(f)$] = $S_\phi(f)$ of the signal plus that of the Ref and the measurement system.

4.3 MEASUREMENT OF SYSTEM NOISE FLOOR

In a real measurement system the PM noise introduced by the DBM, filter and the amplifiers determine the lowest PM noise that can be measured, thus defining a so-called noise floor of the measurement system [4,18]. Figure 6 shows a typical setup for determining the noise floor using PM/AMCAL to determine [K_d G(f)] [20]. Here, the output of a low noise reference oscillator is split into two signals using a reactive power splitter and fed to the two inputs of the DBM at the same level used for the measurements. The measured $S_\phi(f)$ reflects the noise floor of the measurement

system, assuming that the AM noise can be neglected [18]. One has to be careful of-course to make sure that the signal drive level, impedance, electrical lengths of the cables are kept as much as possible, identical for both the actual measurement and that for the noise floor measurement so that the mixer performance is the same for the calibration as for the actual measurement [18].

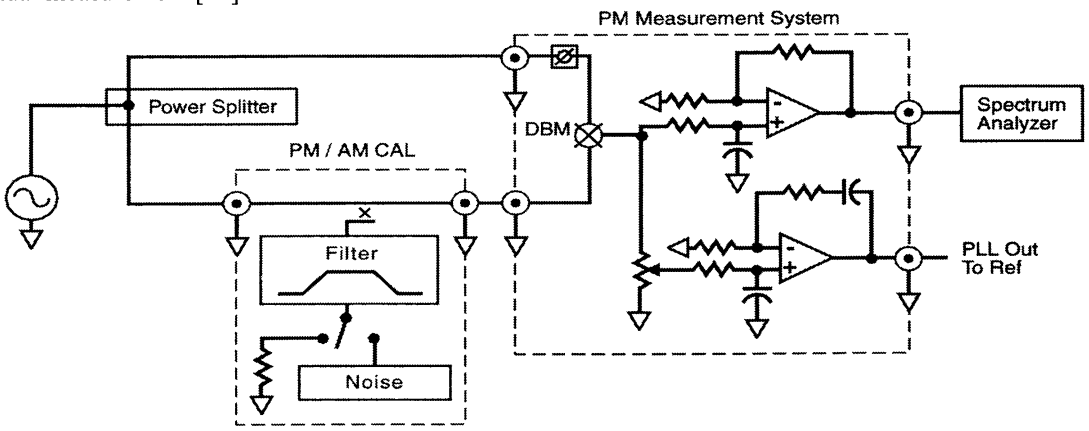

Figure 6. Block diagram of a noise floor measurement using an in-situ calibration standard PM/AMCAL to determine mixer sensitivity and amplifier gain [$K_dG(f)$] with Fourier frequency.

4.4 THREE-CORNER-HAT FOR VERY LOW NOISE OSCILLATORS

The above single-channel measurement systems all have two serious limitations for measuring the PM noise of very low noise sources. These are that in a single-channel system we cannot distinguish between PM noise in the reference and PM noise in the source under test or noise in the measurement system. Fig. 7 shows one method to significantly reduce the noise contributions from both of these sources. This type of measurement setup uses two duplicate systems to drive a cross-correlation spectrum analyzer. The oscillator signals are split with reactive power splitters to provide two pairs of input signals. These signals are connected to two near identical measurement systems. Two independent PLLs lock the two reference oscillators with the oscillator under test. The outputs of both channels are then fed into the cross-correlation FFT spectrum analyzer. The improvement brought about by this technique comes because the noise contributed by the individual mixer-filter-amplifier strings and the two ref oscillators are uncorrelated and average towards 0 in the cross-correlated output. The correlated noise is the actual noise of the input oscillators plus some single-channel noise due to leakage and imperfect isolation in the power splitters. Calibration of the mixer sensitivity-gain product [$K_dG(f)$] is carried out, as before, by introducing a calibrated noise source PMCAL into the common channel and measuring the cross-spectral density. The power spectral density of the cross-correlated signal then gives the PM noise of the oscillator under test. Typically the PM noise from the reference oscillators and the noise floor of the single channel measurement systems are reduced 10 dB to 20 dB over the single-channel measurements. Improvements in noise floor using the cross-correlation technique of-course come with a price. The uncorrelated noise averages towards zero as $N^{-0.5}$, where N is the number of measurements, thus requiring large number of observations [22]. It has been shown in [10] for instance, that the 1-sigma confidence interval for a single channel measurement is about ±10% for 100 measurements. To obtain the same confidence level for PM noise measurement 10 dB below the single channel noise floor using the cross-correlation technique requires about 20,000 measurements.

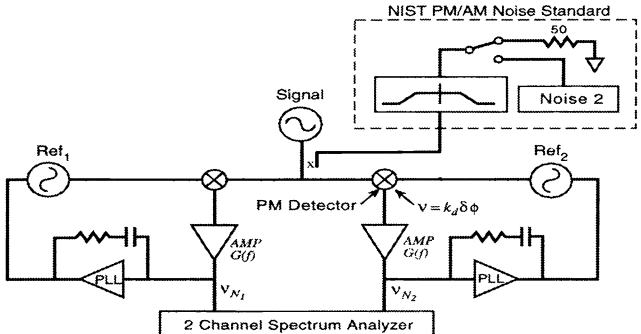

Figure 7. Block diagram of a two-channel PM noise measurement system for two oscillators that uses both an in-situ calibration standard and cross-correlation to reduce the contributions of PM noise in the two references and measurement systems.

4.5 FREQUENCY DISCRIMINATOR TECHNIQUES

Frequency discriminator techniques are often used to measure PM noise in sources that have line widths larger than a few kHz, or cannot be tuned with a PLL circuit, or when only one is available. Figure 10 shows a single-channel PM noise measurement system that uses a delay line as a frequency discriminator. The signal is split with a delay line is placed in one leg and a phase shifter placed in the other leg. The signals from the two legs are then fed into a double balanced mixer. The DC voltage out of the phase detector is proportional to the frequency fluctuations of the source about the point where the phase difference between the two paths is $\pi/2$. One convenient method of calibration is to measure the change in DC voltage from 0 as the frequency of the source is tuned away from this balance point. The PM noise of the source is then given by

$$S_\phi(f) = PSD(V_n) / [K_v f G(f)]^2, \quad (28)$$

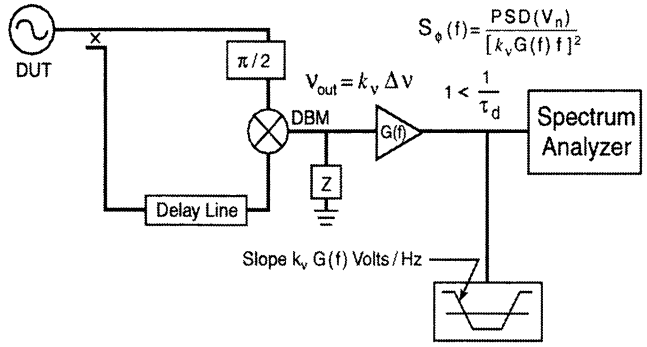

Figure 8. Block diagram of a delay line frequency discriminator used to measure PM noise in a source.

where K_v is the slope of the voltage change with frequency change in Hz. This calibration method is only valid for $f << 1/2\pi\tau_d$, where τ_d is the differential delay between the two arms of the measurement system [4]. Another method, which works over a much wider range of offsets frequencies, is to use PM/AMCAL to determine $[K_v f G(f)]^2$. The resolution of this system for measuring PM noise is degraded from that of a simple single-channel system by the factor $(2\pi f\tau_d)^2$, For τ_d = 500 ns and f=1 Hz, this degradation is approximately 110 dB.

High-Q cavities can also be used as frequency discriminators [4].

4.6 PM NOISE OF OTHER DEVICES

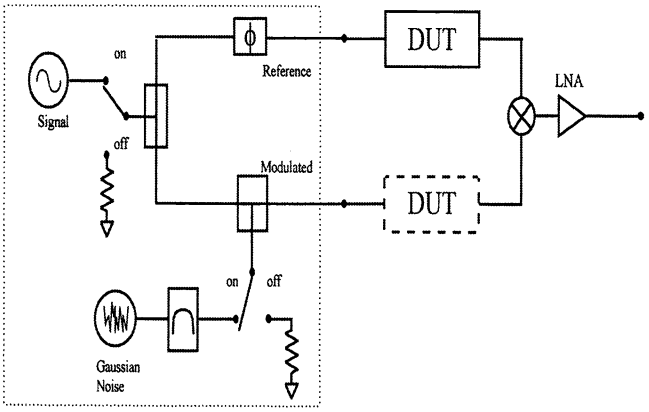

Figure 9. Experimental setup using PM/AMCAL approach to determine the product of mixer sensitivity and gain $[K_d G(f)]$ for measurement of PM noise of a pair of amplifiers or other devices. If the devices do not change the frequency, or introduce a significant delay, then one can measure a single device.

Many times one is required to measure the PM noise introduced by passive devices or circuits using active devices, such as amplifiers, synthesizers, or frequency converters. The typical setup used for such a device under test is shown in Fig. 9. The product of mixer sensitivity and gain can be determined using the beat frequency method with another reference oscillator or using the phase noise standard approach as illustrated here. If the PM noise of the device under test is close to or better than the noise floor of the measurement setup, cross correlation techniques as described in section **4.5** can be used. This setup enables one to typically improve the noise floor by more than 15 dB [18,21]. Another powerful technique is that of carrier-suppression described below in section **4.7**

4.7 PM NOISE MEASUREMENTS USING-CARRIER SUPPRESSION

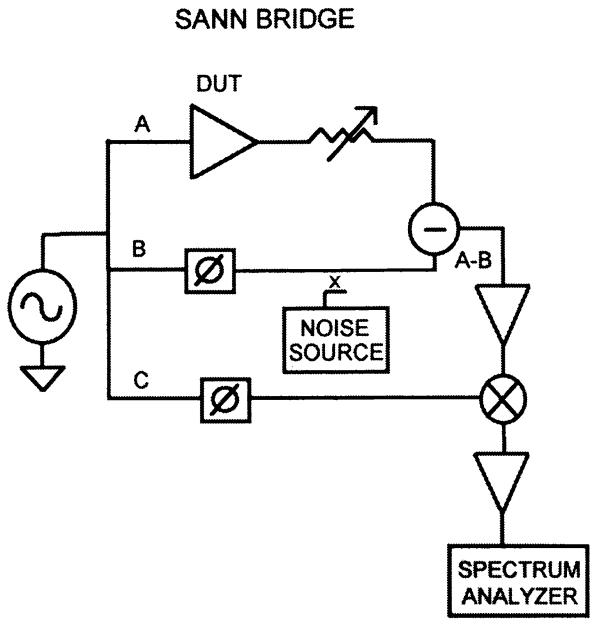

Figure 10. Basic carrier suppressed bridge for measuring AM or PM noise in a device.

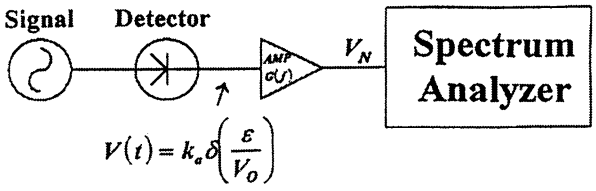

Figure 11. Block diagram of a simple AM noise measurement system.

Figure 10 shows a typical carrier suppression bridge [23-28]. The central feature of this approach is based on fact that the PM and AM noise are defined relative to the amplitude of the carrier. See Eqs. (4) and (8). By reducing the amplitude of the carrier, without affecting the noise sidebands, we can significantly enhance the PM noise. This is schematically shown in Figure 10, where by careful adjustment of the attenuator in arm A and the phase shifter in arm B, the carrier can be suppressed by 50 to 100 dB. The suppressed carrier is then amplified by an amount G. This reduces the effect of the 1/f noise in the detection system approximately a factor of G. PM noise is detected by adjusting the phase shifter to achieve approximately $\pi/2$ rad between the two signals at the mixer. For AM noise detection the signals are in phase at the mixer.

A significant advantage over the cross-correlation approach is that the results are available in real time without the need for a two-channel cross-correlation spectrum analyzer or the need to take long data samples.

The noise floor for measuring PM noise in amplifiers and similar devices is usually much better than that of the two channel cross-correlation approaches at low f where the measurements are limited by 1/f noise in the phase or amplitude detectors. The thermal noise floor is similar to that of other systems [23-28]. The lowest noise floors at 1 to 10 Hz offset are reported in [28] which uses both carrier suppression and cross correlation. Another advantage of carrier suppression is that PM noise measurement systems are approximately a factor G less sensitive to AM noise in the source since the passive differencing element is typically much more linear (has much lower AM to PM conversion) than a mixer. One disadvantage is that the system is critically dependent on a careful balance of the bridge. Typically the carrier is reduced by 50 to 100 dB by the carrier suppression bridge, which can change with time and temperature. The sensitivity of the bridge is very high, making calibration somewhat more difficult than the other systems described above.

5. AM NOISE MEASUREMENT SYSTEM

5.1 SINGLE CHANNEL AM MEASUREMENT SYSTEM

A simple single-channel system for the measurement of AM noise in an oscillator output is shown in Fig.11 [4]. The AM noise on the oscillator output is demodulated using an AM detector, amplified using a low noise amplifier and fed to a spectrum analyzer. The input noise voltage to the spectrum analyzer is given by

$$V_n(t)= K_aG(f)\,\Delta(\varepsilon/V_0), \tag{29}$$

where K_a is the AM detector sensitivity and G(f) is the amplifier gain. The power spectral density of V_n measured by the spectrum analyzer yields $S_a(f)$ by the relation

$$S_a(f)= \text{PSD}\,(V_n) / [K_aG(f)]^2. \tag{30}$$

Calibration of the product $K_aG(f)$ can be performed using a signal source with AM capability operating at the same carrier frequency and power level. If we use the calibrating signal amplitude modulated with a single frequency, say 1 kHz, and modulation index AM%. The power in the modulation signal component at the input of the detector is ½(AM%/100). If the power of this component measured in the spectrum analyzer is called, "AM reference level" then we have the following relation

$$[K_aG(f)]^2 = (\text{AM reference level})^2 / (½(\text{AM\%}/100)). \tag{31}$$

5.2 TWO-CHANNEL AM MEASUREMENT SYSTEM

The above method AM noise measurement suffers from the usual drawback that it is not possible to separate the contributions from the system, the detector and amplifier in the measured $S_a(f)$ [4]. Thus when making very low AM noise measurements one usually makes use of a cross correlation setup which uses two identical channels and a two channel cross correlation spectrum analyzer similar to that shown in Fig. 7 for PM noise measurements. In this case the uncorrelated noise in the AM detectors averages to 0 as $N^{-0.5}$, where N is the number of measurements. With this improvement comes the need for much longer averaging times. Calibration can also be accomplished using PM/AMCAL in a manner identical to that used in Figs. 7 or 9 [20, 21].

5.3 AM NOISE MEASUREMENTS USING-CARRIER SUPPRESSION

Figure 10 shows a typical carrier suppression bridge [23-28]. The central feature of this approach is based on fact that the PM and AM noise are defined relative to the amplitude of the carrier. By reducing the amplitude of the carrier, without affecting the noise sidebands, we can significantly enhance the PM and AM noise. This is schematically shown in Figure 10, where by careful adjustment of the attenuator in arm A and the phase shifter in arm B, the carrier can be suppressed by 50 to 100 dB. The suppressed carrier is then amplified by an amount G. This reduces the effect of the 1/f noise in the detection system approximately a factor of G. AM noise is detected by adjusting the phase shifter to achieve approximately 0 rad between the two signals at the mixer.

A significant advantage over the cross-correlation approach is that the results are available in real time without the need for a two-channel cross-correlation spectrum analyzer or the need to take a long data samples. The noise floor for measuring AM noise in oscillators, amplifiers, and similar devices is usually much better than that of the two channel cross-correlation approaches at low f. Another advantage is that the AM noise in the source is highly cancelled by the passive differencing element. The disadvantage is that the system is critically dependent on a careful balance of the bridge. Typically the carrier is reduced by 50 to 100 dB by the bridge, which can change with time and temperature. The sensitivity of the bridge is very high, making calibration somewhat more difficult than the other systems described above.

6. TYPICAL RESULTS AND DISCUSSION

To illustrate the above descriptions of the PM and AM noise determination techniques, we present in this section some typical results of measurements. Figure 12 shows some data taken with the NIST PM/AM noise standard [20,21]. See Figs. [5] and [6]. Curve A shows the measured PM noise of a high performance 100 MHz oscillator. Note that the PM noise close to the carrier, which in this case is due to noise in the quartz resonator, falls as f^{-3}. The broadband noise originates from the finite power level of the oscillator signal and the noise figure of the sustaining amplifier. Trace B shows the level of noise injected into the measurement system when PM/AMCAL is "ON". This is used to calibrate the gain of the mixer and amplifier. Trace C shows the typical noise floor of a two channel PM noise measurement system at 100 MHz using cross correlation [20-22].

Figure 13 shows the AM and PM noise of a 10.6 GHz oscillator. Again note that close to the carrier the PM noise falls as f^{-3}. The AM noise falls as roughly 1/f. The PM noise of amplifiers and mixers close to the carrier typically show a 1/f dependence.

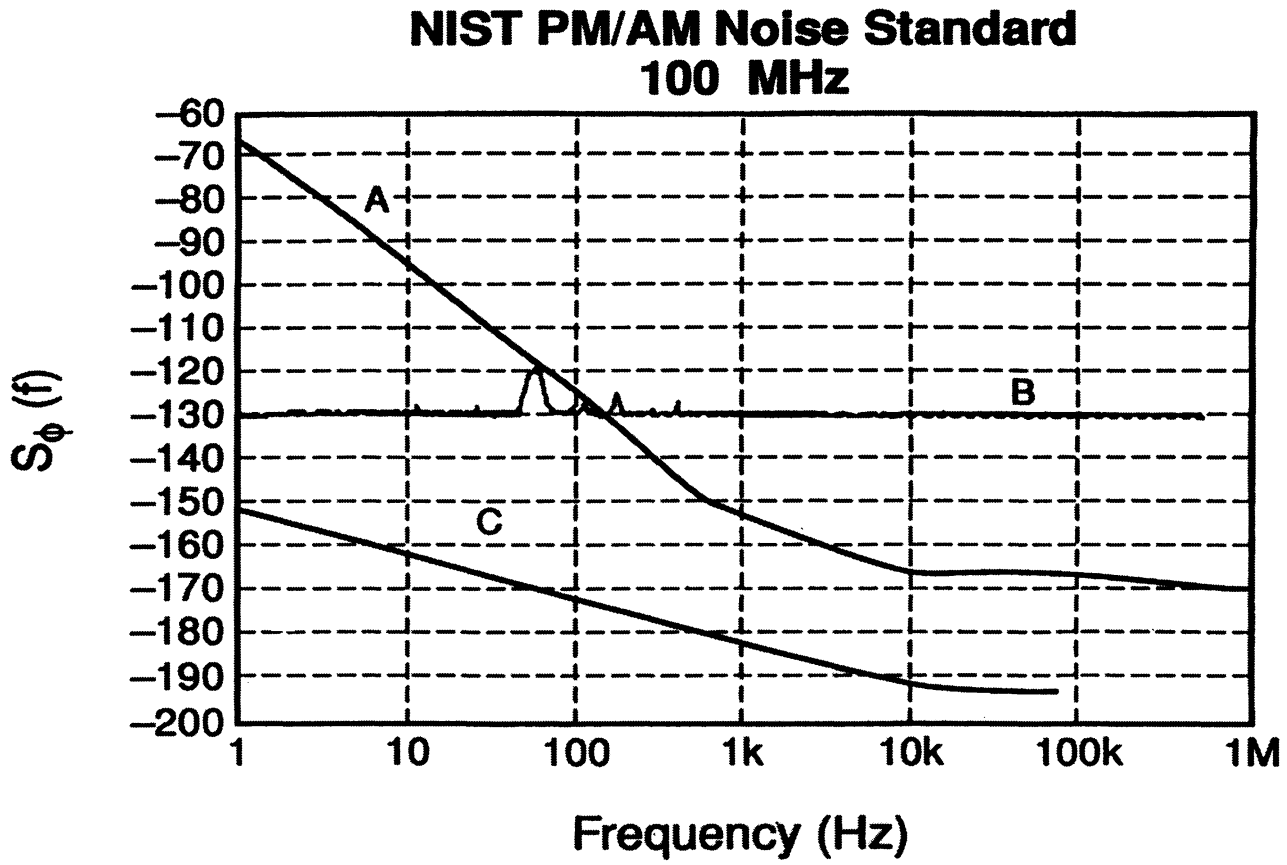

Figure 12. Data taken with NIST PMAMCAL standard. See text for details.

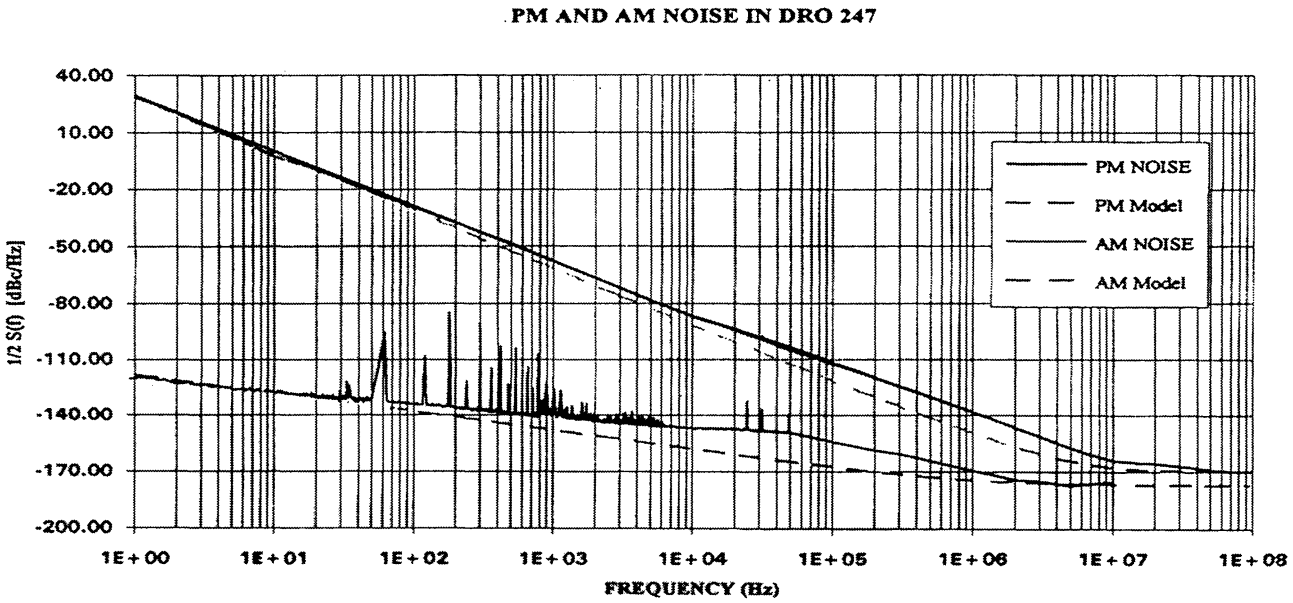

Figure 13. PM and AM noise of a 10.6 GHz DRO.

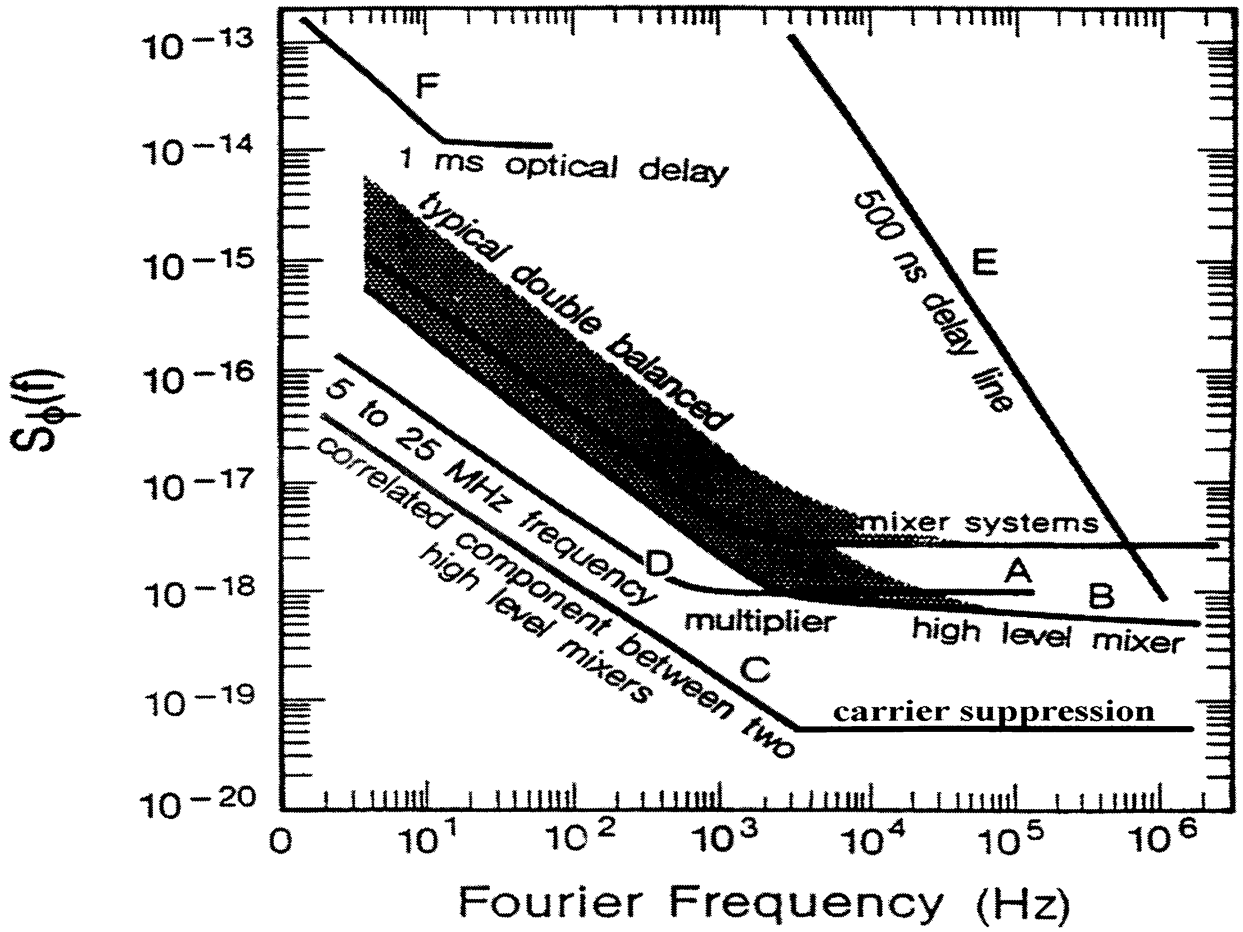

Figure 14. Approximate noise floor for different measurement techniques at frequencies below 1 GHz.

Finally, we show in Fig. 14 a comparison of the approximate PM noise floor for the different techniques. Both carrier suppression and cross-correlation techniques yield noise floors which approach the thermal noise floor of -193 dBc/Hz for a carrier power of + 16 dBm as described earlier, thus enabling the most accurate broadband measurements. Carrier suppression techniques are much faster because the results are avail in near real time [24-28].

7. CONCLUSION

In this paper we have attempted to give a brief review of the fundamental concepts of PM and AM noise metrology. We have also described the different state-of-the-art techniques to measure them. Some typical results of actual measurements by the author and collaborators have been discussed for illustration. We conclude by mentioning that the description in the present paper is obviously not very detailed and the reader is referred to the extensive literature cited.

8. ACKNOWLEDGEMENTS

I thank Eva Ferre-Pikal, Craig Nelson, Amitava SenGupta, and David Howe for many helpful discussions.

9. REFERENCES

[1]. J.A. Barnes, A.R. Chi, L.S. Cutler, D.J. Healy, D.B. Leeson, T.E. McGuinal, J.A. Mullen Jr., W.L. Smith, R.L. Sydnor, R.F.C. Vessot and G.M. Winkler, "Characterization of frequency stability," Proc. IEEE Trans on I&M, **20**, 105-120, 1971. Also in [2]

[2]. D.B. Sullivan, D.W. Allan, D.A. Howe and F.L. Walls Eds, "Characterization of clocks and oscillators," NIST Tech note **1337**, 1990.
[3]. E.S. Ferre-Pikal, J.R. Vig, J.C. Camparo, L.S Cutler, L. Maleki, W.J. Riley, S.R. Stein, C. Thomas, F.L. Walls, and J.D. White, Draft Revision of IEEE Std 1139-1988 "Standard Definitions of Physical Quantities for Fundamental Frequency and Time Metrology - Random Instabilities," Proc. 1997 IEEE Intl. Freq. Contr. Symp., 338-357, Orlando, FL, 1997.
[4]. F.L. Walls and E.S. Ferre-Pikal, "Measurement of Frequency, Phase Noise and Amplitude Noise," *Wiley Encyclopedia of Electrical and Electronics Engineering*, **12**, 459-473, 1999.
[5]. W.F. Walls and F.L. Walls, "Computation of the time-domain frequency stability and jitter from PM noise measurements," Proc. 2001 IEEE Intl. Freq. Contr. Symp. 161-166, Seattle, WA, 2001.
[6]. F.L. Walls and A. DeMarchi, "RF spectrum of a signal after frequency multiplication; measurement and comparison with a simple calculation," IEEE Trans. I &M, **24**, 210-217, 1975.
[7]. F.L. Walls, "Correlation between upper and lower sidebands," IEEE Trans. UFFC, **47**, 407-410, 2000.
[8]. F.L. Walls, E.S. Ferre-Pikal, and S.R. Jefferts, "The origin of 1/f PM and AM noise in bipolar junction transistor amplifiers," IEEE Trans. UFFC, **44**, 326-334, 1997.
[9]. A. Hati, D. Howe, D. Walker, and F. L. Walls, "Noise figure vs PM noise measurements: a study at microwave frequencies," to be publish in the joint 2003 IEEE Freq. Contr. Symp. and Europ. Freq. and Time Forum, Tampa, FL., 2003.
[10]. F.L. Walls, D.B. Percival, and W.R. Irelan, "Biases and variances of several FFT spectral estimators as a function of noise type and number of samples," Proc. 43rd Ann. Symp. Freq. Cont., 336-341, Denver, CO, 1989. Also in [2].
[11]. D.W. Allan, "Statistics of atomic frequency standards," Proc. IEEE, **54**, 221-230, 1966.
[12]. L.S. Cutler and C.L. Searle, "Some aspects of the theory and measurement of frequency fluctuations in frequency standards," Proc. IEEE, **54**, 89-100, 1966.
[13]. J.A. Barnes and D.W. Allan, "Variances based on data with dead time between the measurements," NIST Tech Note **1318**, 1990. Also in [2].
[14]. F.L. Walls, John Gary, Abbie O'Gallagher, Roland Sweet and Linda Sweet, "Time Domain Frequency Stability calculated from the frequency domain description," NIST report, **NISTIR-89-3916**, 1989.
[15]. D.A. Howe, "The total deviation approach to long-term characterization of frequency stability," IEEE Trans. UFFC, **47**, 1102-1109, 2000
[16]. Stable 32 is Available form Hamilton Technical Services, 195 Woodbury St.,S. Hamilton, MA 01982, USA.
[17]. A. SenGupta and F.L. Walls, "Effect of aliasing on spurs and PM noise in frequency dividers," Proc. Intl. IEEE Freq. Cont. Symp., 541-548, Kansas City, MO, 2000.
[18]. F. L. Walls, A. J. D. Clements, S. M. Felton, M. A. Lombardi, and M. D. Vanek, "Extending the range and accuracy of phase noise measurements," Proc. 42nd Ann. Symp. on Freq. Cont., 432-441, Baltimore, MD, 1988.
[19]. F.L. Walls, "PM and AM noise of combined sources" to be publish in the 2003 IEEE Joint Freq. Contr. Symp. And Europ. Freq. and Time and Forum, Tampa, FL, May 2003.
[20]. F L. Walls, "Secondary standard for PM and AM noise at 5, 10 and 100 MHz," IEEE Trans. I&M, **42**, 136-143, 1993.
[21]. F.L. Walls, "Reducing errors, complexity and measurement time of PM noise measurements," Proc. 1993 Intl. IEEE Freq. Contr. Symp.," 289-297, Salt Lake City, UT, 1993.
[22]. W.F. Walls, "Cross correlation phase noise measurements," Proc 1992 IEEE Freq. Cont. Symp. 257-261, Hershey, PA, 1992.
[23]. E.N. Ivanov and F.L. Walls, "Interpreting AM and PM noise measurements in two-channel interferometric measurement systems,", Proc. 14th Europ. Freq. and Time Forum, 118-122, Torino. IT, 2000
[24]. A. De Marchi, F. Andrisani, and G.P. Bava, "Noise limits of cross-correlation two-channel noise measurement systems," Proc. 14th Europ. Freq. and Time Forum, 123-128, Torino, IT, 2000
[25]. F.L. Walls, "Suppressed carrier based PM and AM noise measurement techniques," Proc. 1997 IEEE Int. Freq. Contr. Symp., 485-492, Orlando, FL, 1997.
[26]. E.N. Ivanov, M.E. Tobar and R.A. Woode, "Applications of interferometric signal processing to phase noise reduction in microwave oscillators," IEEE Trans. MTT, **46**, N10, 1537-1546, 1998.
[27]. E.N. Ivanov, M.E. Tobar and R.A. Woode, "Microwave interferometry: application to precision measurements and noise reduction techniques," IEEE Trans. UFFC, **45**, 1526-1537, 1997.
[28]. E. Rubiola and V. Giordano, "Correlation-based phase noise measurements, RSI, **71**, 3085-3091, 2000.